Ind. J. Pharm. Edu. Res., 2025; 59(2):585-601.
https://www.ijper.org

Original Article

Formulation and Evaluation of Lipid Nanogel Loaded with Quercetin and Curcumin for Improvement of Topical Bioavailability

Mohammad Kashif Iqubal[1,2], Shadab Md[3], Javed Ali[1,*], Sanjula Baboota[1,*]

[1]Department of Pharmaceutics, School of Pharmaceutical Education and Research, Jamia Hamdard, New Delhi, INDIA.
[2]Department of Pharmaceutical Sciences, Irma Lerma Rangel School of Pharmacy, Texas A and M Health Science Center, Texas A and M University, College Station, TX, USA.
[3]Department of Pharmaceutics, Faculty of Pharmacy, King Abdulaziz University, Jeddah, SAUDI ARABIA.

ABSTRACT

Aims: The present work was aimed to develop and optimize the QCN and CRN-loaded combinatorial NLC (QC-NLC) gel through the Central Composite Rotatable Design (CCRD) for bioavailability improvement of QCN and CRN in the management of skin cancer after its topical application. **Materials and Methods:** After the compatibility study and selection of excipients, CCRD was run and thirteen formulae were obtained. Optimization was completed against particle size, PDI and entrapment efficiency. QC-NLC nanogel was prepared from the optimized combinatorial NLC formulation and evaluated on different parameters, such as homogeneity, spreadability, extrudability, pH, drug content, drug release, permeation, dermatokinetic, stability, etc., **Results:** Developed combinatorial NLCs were optimized based on the particle size (163.8±1.5 nm), PDI (0.28±0.04), and surface charge of optimized NLC was recorded -31.6±1.4 mV. TEM image showed spherical-shaped particles. NLC-based nanogel showed a pH of 6.93±0.59, drug content of 100.85±4.07% QCN and 98.41±5.15% CRN and it exhibited a smooth homogenous characteristic. The nanogel demonstrated a lower value of extrudability than conventional gel, which offers an advantage over the conventional gel. The release profile showed higher drug release from nanogel in a prolonged manner. The permeation and dermatokinetic studies exhibited higher flux and drug distribution ability in the epidermis and dermis layers of skin than conventional gel and it has been further confirmed by the depth analysis using confocal microscopy. Stability studies showed a surpassing storage ability of developed nanogel. **Conclusion:** The topically applied developed nanogel could be a potential approach for skin cancer treatment due to its appreciably improved bioavailability ability in the layers of skin.

Keywords: Combination therapy, Dermatokinetics, Design of experiment, Extrudability, Lipid nanocarrier.

Correspondence:
Dr. Javed Ali
Department of Pharmaceutics, School of Pharmaceutical Education and Research, Jamia Hamdard, New Delhi, INDIA.
Email: jali@jamiahamdard.ac.in

Dr. Sanjula Baboota
Department of Pharmaceutics, School of Pharmaceutical Education and Research, Jamia Hamdard, New Delhi, INDIA.
Email: sanjulababoota19@gmail.com

Received: 11-08-2024;
Revised: 08-12-2024;
Accepted: 05-02-2025.

INTRODUCTION

The skin is the body's largest, heaviest and outermost organ. It is made up of three stratified tissue layers: the dermis, the epidermis and the subcutaneous tissue.[1] The outermost layer of skin, known as the epidermis, is made up of a variety of tissues and cells, including melanocytes, basal cells, keratinocytes and squamous cells. Furthermore, the skin structure contains several skin appendages, such as hair follicles, sweat glands, sebaceous glands and nails.[2] Skin, being the 1st line protection barrier of the body, is directly exposed to environmental toxins, chemical toxins and ultraviolet radiation, resulting in the manifestation of various problems like erythema, wrinkles, edema, immunosuppression, photoaging, sunburn and skin cancers. According to recent reports, skin cancer is the most frequent cancer, with over a million new cases occurring globally each year. More people get skin cancer than any other type of cancer combined. Based on their clinical behavior and the cells from which they originate, the various forms of skin cancer are categorized. The most common types of Skin Cancer are Melanoma and Nonmelanoma (NMSC), which also include Squamous Cell Carcinoma (SCC) and Basal Cell Carcinoma (BCC). Furthermore, the WHO reported that the incidence of melanoma NMSC has increased during the past few decades. Presently, 1-3 million NMSC and 1,32,000 melanomas are reported annually worldwide.[3,4]

Due to the major problems associated with the use of anti-cancer drugs, such as multidrug resistance and the involvement of

DOI: 10.5530/ijper.20250569

multiple pathways in the development of cancer cells, the current focus of research has shifted towards the use of combination cancer therapy. This treatment involves the simultaneous administration of two or more anticancer drugs in a single vehicle, which results in providing synergistic or additive effects as compared to monotherapy.[4,5] Combination cancer therapy acts by modulating multiple signaling pathways, suppressing MDR, reducing individual drug-related toxicity, overcoming the shortcomings of each other and reducing the dose of each other, thereby maximizing the treatment effect.[6,7]

Phytopharmaceuticals are gaining immense popularity in treating skin cancer due to the enhanced benefits, mainly in terms of the minimal side effects that they offer over synthetic drugs.[8,9] Numerous studies have shown that the best medications for treating various cancer kinds are Quercetin (QCN) and Curcumin (CRN) together.[10-17] Individually QCN downregulates NF□B, COX-2, EP3, EP4, PCNA and cyclin D1 expressions.[18,19] It also reduces the event of DNA damage by lowering lipid peroxidation.[20] QCN also can work synergistically with other antioxidant systems in the body to decrease oxidative stress.[21] On the other hand, CRN inhibits STAT3 and NF-κB pathways, which are essential for the initiation and spread of skin cancer. Additionally, it has been proposed that in CL-5 xenograft tumors, CRN can trigger apoptosis and down-regulate EGFR, Akt, cMET and cyclin D1. Thus far, it has been shown that CRN possesses anti-skin cancer properties by preventing cell division, stopping the cell cycle and inducing apoptosis through the manipulation of many transcription factors, including AP-1, β-catenin, Notch-1, Hif-1, Erg-1, p53 and PPAR-α.[22,23]

Further, in combination, QCN and CRN can synergistically inhibit skin cancer and show greater potency as compared to when they were given alone. The synergistic mechanism of quercetin and curcumin in skin cancer is modulated by their comprehensive multifactorial mechanism of action. Since both quercetin and curcumin are plant derivates/natural bioactive/polyphenols, they possess potent antioxidants and are anti-inflammatory. They also target distinct as well as overlapping pathways, resulting in enhanced anticancer effects when used in combination. Both molecules inhibit the production of ROS, stimulate the antioxidant effect of SOD and CAT and regulate the transcription and translation of Nuclear factor erythroid-2-related factor 2 (Nrf2) that eventually reduces DNA damage and increases DNA repair.[24,25] These natural bioactives, when used in combination, manifest into doublet inhibition of NF-κB nuclear translocation and other proinflammatory pathways. Also, Quercetin causes apoptosis induction via the regulation of Bax and Bcl-2 through mitochondrial pathways, whereas curcumin causes activation of caspases and also causes downregulation of survival oncogenic pathways such as PI3K/Akt and STAT3.[24,25] Hence, when used in combination, it results in increased pro-apoptotic and anticancer effects. Studies have also shown that quercetin causes the arrest of the G1 phase via Cyclin-Dependent Kinases (CDKs), whereas curcumin primarily causes the arrest of the G2/M phase via modulation of the level of CDK1 and cyclin B1.[26,27] Therefore, when used in combination, it results in increased pro-apoptotic and anticancer effects. Since angiogenesis is one of the pivotal mechanisms in tumor progression and metastasis, when both molecules are used in combination, it causes inhibition of Endothelial Growth Factor (VEGF) and Matrix Metalloproteinases (MMPs) and ultimately causes impairment in newer blood vessel formation and supply of nutrients to tumors.[24,25] Furthermore, quercetin functions as an inhibitor of Histone Deacetylase (HDAC), while curcumin modulates DNA methylation; their combination results in synergistic activation of the tumor suppressor gene.[28,29] Hence, it can be concluded that when quercetin and curcumin are used in combination, they target multiple hallmarks of oncogenic pathways such as NFkB/Nrf2, PI3K/Akt/mTOR/STAT, p53/MAPK/MMP/TGF-β, VEGF/HIF-α, etc. and eventually result in enhanced or improved effects in skin cancer, in contrast to when used individually.[30] Therefore, this combination can result in great efficacies of both the incorporated drugs within a single formulation. Combining two medications into one formulation should increase efficacy and enhance patient compliance, but doing so comes with several difficulties and is not a simple process.[7] However, some lipid-based combination nanoformulations of QCN and CRN have been reported for the treatment of brain diseases,[31] antioxidants,[32] antibacterial[33] and breast cancer.[32] Whereas this research work reports a new topical nanoformulation for the management of skin cancer. The topical approach reduces both the associated advantage of medication targeting and needless cytotoxicity to normal, healthy cells. Additionally, because this route avoids the 1st pass metabolism linked to both medicines, it offers greater bioavailability. It is an efficient, safe, non-invasive and useful method of administering medicine.[33] Since their nanosize guarantees tight contact with the stratum corneum, Nanostructured Lipid Carriers (NLC) are very helpful for topical application, thereby improving the drug flow through the skin.[34] Furthermore, topical NLC treatment forms a monolayer lipid film on the skin that stops Trans Epidermal Water Loss (TEWL), improving skin hydration and moisture content while also boosting the quantity of medication absorbed by the skin.[35,36] Thus, combinatorial NLC enhanced the topical bioavailability of QCN and CRN after application over the skin.

In the present work, QCN and CRN Loaded Combinatorial NLC (QC-NLC) were developed and optimized for the management of skin cancer through the central Composite Rotatable Design (CCRD) by using Design expert software (version 11.1.1.0, State-Ease Inc., Minneapolis, USA). Further, optimized combinatorial QC-NLC-loaded nanogel was prepared and characterized. The novelty of this work from other past studies discussed the *in vitro* and *ex vivo* release, permeation and dermatokinetic characteristics of combinatorial nanogel and

conventional gel. These evaluation parameters determined the improved topical bioavailability of QC-NLC-loaded nanogel. This study also describes the stability profile of nanogel.

MATERIALS AND METHODS

Materials

Quercetin and stearic acid were from Sigma Aldrich (Bengaluru, India), whereas curcumin was obtained from GLR Innovations, New Delhi, India. Turmeric oil was purchased from Kazima Perfumers, Delhi, India. Other excipients such as Labrafil M1944 CS, Labrafil M2125, Labrafac 1349 CS, Captex 355 GPR, Emulcire 61WL2659, Apifil, Cremophore RH 40, Cremophore EL, Gelucire 43/01, Labrafil M2130CS, Compritol ATO 888, Tefose 1500 and Precirol ATO 5 were from Gattefose India Pvt Ltd (Mumbai, India). Capmul MCM and Poloxamer 188 were used by Abitec Corporation, Columbus, USA and BASF East Asia Regional Headquarters Ltd., Quarry Bay, Hong Kong, respectively. Tween 80 was procured from Sisco Research Laboratories Pvt. Ltd (Maharashtra, India) and Tween 20 was obtained from S D Fine Chemicals Ltd., (Mumbai, India). Span 20 and methanol were obtained from Merck (Mumbai, India).

Methods Implemented

Compatibility Study

To ascertain QCN and CRN's compatibility, the two drugs were precisely combined in a 1:1 ratio (5 mg of each). For 28 days, the combination was stored in a vial in a stability chamber at 25±2°C and 60±5% RH. Visual inspection, Differential Scanning Calorimetry (DSC) analysis and FTIR spectra analysis were used to verify the interactions between the medications.[37]

Selection of Suitable Excipients

By adding excess quantities to 1 mL of oil in tiny vials, the solubility of quercetin and curcumin was checked independently in a variety of liquid lipids, including Labrafil M1944 CS, Labrafac 1349, Labrafil M2125 CS, Capmul MCM, Captex 355 GPR and Turmeric oil. To achieve equilibrium, the vials were continually and firmly shaken in a shaker for 72 hr at 25°C. After 72 hr, mixtures were centrifuged in a high-speed centrifuge for 30 min at 37°C at 12000 rpm. The supernatant, after separation and dilution with methanol, the solubility of QCN and CRN was then measured spectrophotometrically (UV spectrophotometer, UV-1601, Shimadzu, Japan) at wavelengths of 257 nm and 417 nm, respectively.[35]

By adding the drugs in gains of 5 mg to 1 g of melted solid lipids (Emulcire 61WL2659, Apifil, Precirol ATO 5, Stearic acid, Gelucire 43/01, Compritol ATO 888, Labrafil M2130CS, Tefose 1500), at above 20°C of its melting point, the appropriate solid lipid was picked based on the best solubility of QCN and CRN. The medication was added to the lipids repeatedly until it was no longer able to dissolve. The quantity of QCN and CRN that got solubilized in the lipids was calculated by visual examination of the mixture. The experiment was conducted in triplicate. Further, the compatibility of selected solid lipids and liquid lipids was performed for their physical compatibility. A glass tube was filled with the Binary Mixture of Lipid (BML) in the ratio of 1:1. The blend was liquefied at 70°C, combined and allowed to cool until it reached room temperature. The cooled congealed lipid substance in the glass tubes was then visually examined under bright light to check for any distinct layers.[38]

To determine their miscibility, the liquid and solid lipids with the highest solubilizing capability for QCN and CRN were mixed in the ratios of 90:10, 85:15, 80:20, 70:30 and 60:40. Next, the BML was stirred on a magnetic stirrer at 200 rpm for 1 hr at 85°C. To find out if the two components were miscible, a cold sample of the combined solid and liquid lipid was placed on filter paper as a smear. The mixture that showed a melting point over 40°C and did not show any traces of liquid lipid on the filter paper was chosen for the creation of QC-NLC.[39] Based on their ability to emulsify the chosen BML, surfactants were chosen. The surfactant's ability to emulsify the optimized BML has been adapted from the technique that Negi *et al.* (2014) reported.[40] In short, 100 mg of BML was dissolved in 3 mL of methylene chloride. Next, 10 mL of a 5% w/v aqueous surfactant solution was added and everything was kept at the same temperature. Magnetic stirring was employed for mixing the resulting slurry. After that, the mixture was heated to 40°C to get rid of the extra methylene chloride. After diluting 1 mL of the combination with 10 mL of filtered water, the %transmittance was measured in triplicate at 25°C, after dilution, by UV spectrophotometry at 510 nm.[40]

Optimization and Selection of a Formula for QC-NLC Using CCRD

The melt dispersion method was used to prepare combinatorial QC-NLC dispersion, which was then ultrasonically processed. The effects of BML and surfactant concentrations on particle size, Polydispersity Index (PDI) and Entrapment Efficiency (EE) were measured using CCRD. Table 1 displays the limits of the independent variables. Initial trials were used to determine the range of independent variables. Table 2 describes the design arrangement of various runs produced by the software. Thirteen of the suggested formulae by the design were prepared. For the formulation, the optimized ratio of BML of Precirol® ATO 5 and turmeric oil was prepared, this resultant mixture was heated at 80°C to melt it completely in a separate beaker by magnetic stirring maintained at 80°C with 600 rpm. After that 4 mg QCN and 8 mg CRN were added in the melted oily phase.

Cremophore® RH 40 was solubilized in a small amount of double-distilled water at 80°C and 600 rpm to create the aqueous phase, which was then gradually increased to the desired final volume. At 80°C and 700 rpm, the resultant aqueous solution was continuously stirred while being distributed dropwise in an oily

phase. This mixture was agitated at 1000 rpm for 2 hr at 80°C. With a probe sonicator, the crude dispersion was subjected to 80 sec of sonication. The QCNLCs were assessed for EE, PDI and particle size. The acquired data was subjected to ANOVA analysis and 3D response surface methods were utilized to examine the impact of independent variables on responses. After that, the aim of response variables was specified and a numerical optimization technique was used.

Particle Size and Polydispersity Index (PDI) Determination

Using a Zetasizer, the particle size and PDI of the dispersions of combinatorial QC-NLCs were determined. A homogeneous dispersion was obtained by diluting the NLC dispersion in double distilled water at a ratio of 1:100. At 25±2°C, the viscosity and refractive index of the water employed as a dispersant were 0.9 cP and 1.3, respectively. The mean particle size was calculated by averaging the three data.[41]

Determination of Entrapment Efficiency

5 mL of QC-NLC were placed into a centrifuge tube and centrifuged using ultracentrifuge (Beckman Coulter India Pvt. Ltd.,) at 40,000 rpm for 60 min at 10°C. After being separated, the supernatant was diluted with methanol and subjected to filtration through 0.45 µm filter paper. The filtrates were subjected to UV spectrophotometry at 25±2°C, with the QCN and CRN contents measured at 257 nm and 417 nm, respectively. Using the provided equation 1, the percent entrapment efficiency was determined, where Ws is the quantity of QCN/CRN in the supernatant following centrifugation and Wd is the total amount of QCN/CRN added in the nanosystem.

Equation 1 $\%EE=(Wd-Ws)/Wd\times100$

Evaluation of Surface Charge

Zetasizer was used to do the zeta potential study in triplicate. Zeta potential was determined by diluting approximately 50 µL of the sample with 10 mL of distilled water. Every measurement was done at 25±2°C.

Evaluation of Surface Morphology

Transmission Electron Microscopy (TEM) was used to assess the surface morphology of combinatorial QC-NLC. The samples were diluted 50 times with water and then a drop was placed on the grid and left for a minute. By using the corner of a piece of filter paper to absorb the drop, the leftover NLC was eliminated. After that, the grid was left with a 1% phosphotungstate drop for 10 sec. After removing the leftover solution using a piece of filter paper to absorb the liquid, the samples were allowed to air dry before being analyzed by TEM.[42]

Preparation of Combinatorial QC-NLC Loaded Nanogel and Conventional Gel Formulation

QC-NLC-based nanogel was prepared with carbopol 934 gel at a concentration of 0.5% w/w that was able to provide proper consistency of the drug-loaded NLC gel. The prepared optimized QCNLC (10 mL) was kept in a beaker and then a sieved weighed quantity of carbopol 934 was transferred into the beaker slowly while continuously stirred at 1200 rpm and at a temperature of 50°C. Next, prepared dispersions were permitted to overnight swelling on the magnetic stirrer. Finally, neutralization with the addition of triethanolamine (0.05% w/w) yielded the gel. Identical to the previous method was used for the preparation of optimized conventional gel of QCN and CRN. But in this case, both the drugs were first dispersed in ethanol, then added into the swelled semi-solid mass of carbopol 934 (1.0%) and finally subjected to neutralization with the addition of triethanolamine (0.05% w/w) until yielding the gel.[37]

Determination of Homogeneity, Spreadability, Extrudability and pH

By pressing a small amount of sample between the thumb and index finger, it was possible to assess the consistency and homogeneity of the gel by noting any particles present on the finger. There wouldn't be any gritty particles at all in a homogenous gel, which would provide a smooth feel between the fingertips. When 20 g of gel was placed in an aluminum collapsible tube, the weight (g) needed to extrude at least a 0.5 cm ribbon of gel in 10 sec was used to calculate the extrudability (g/cm^2) of both conventional and nanogel.[43] The experimentation in triplicate was followed by calculations using Equation 2:

$$\text{Extrudability} = \frac{\text{Applied weight to extrude formulation from syringe (g)}}{\text{Area (cm)2}} \quad \text{.....Equation 2}$$

To test the gel's spreadability, two glass plates (9×2 inches) were sandwiched with 1 g of gel sample (nanogel and regular gel separately). After that, the glass plate was subjected to a 200 g weight for 5 min. After applying weight, the area that each gel covered was computed and compared. After dissolving 1 g of nanogel and conventional in 100 mL of distilled water, the mixture was kept for 2 hr. After fully submerging the electrodes

Table 1: Independent factors used in design for preparation QC-NLCs.

Factors	Levels used	
Independent variables.	Low	High
A [Lipid concentration (%w/v)].	1	3
B [Surfactant concentration (%w/v)].	2	5
Dependent variables.	Constraint	
R1 [Mean particle size (nm)].	Minimum	
R2 [PDI].	Maximum	
R3 [Entrapment efficiency (%)].	Maximum	

of a calibrated digital pH meter (Mettler Toledo, Mumbai, India) in the gel dispersion, the pH was measured in triplicate at 25°C.[44]

Determination of Drug Content

Combinatorial QC-NLC nanogel weighing 100 mg was removed from the container's top, middle and bottom. Methanol was used to dissolve the materials in individual conical flasks. After 3 hr of shaking the flasks using a mechanical shaker, the solution was filtered and diluted with methanol. At 257 nm and 417 nm, the solution's absorbance was measured and compared to a placebo gel methanolic solution, which was used as a reference.

Determination of Occlusive Properties

Two separate 100 mL beakers containing water (50 mL) each were sealed with cellophane tape, filter paper and cover. Gel weighing 10 mg/cm^2 was evenly placed over the filter paper and left 288 for 48 hr at 32°C and 50-55% relative humidity. A beaker filled with filter paper devoid of gel was used as a point of comparison. Equation 3 was used to calculate the occlusion factor (F) after 290 48 hr, where A and B are the loss of water without and with the samples, respectively.[45]

Equation 3:

$$A\text{-}B/A\times100$$

Texture Analysis of Gels

For texture profile analysis, approximately 50 mL of the prepared gels were taken in a 100 mL beaker and were ensured to be completely free from the presence of air bubbles and have a smooth surface. The gel was then compressed twice to a depth of 15 mm at a rate of 2 mm/s using an analytical probe, with a 2-sec pause between the end of the first compression and the start of the second. The software-regulated texture analyzer used for the analysis was called TA.XT Plus 298 Texture Analyzer. The curve that was produced after the research showed the mechanical properties of the gels, including their cohesiveness, consistency, hardness and index of viscosity.[46]

In vitro Drug Release Study

The Franz diffusion cell, which has a surface diameter of 0.785 cm^2, was used in this work. A dialysis membrane with a MWCO between 12,000 and 14,000 Da was collected and fastened between the donor and receptor compartments.[38] Subsequently, a dialysis membrane was coated uniformly with 1 g of combinatorial nanogel and conventional gel. The methanolic Phosphate Buffer Solution (mPBS) in the receptor compartment had a pH of 7.4 and was kept at a constant 37±2°C. Throughout the investigation, mPBS was stirred at a 500-rpm speed. At intervals of 0, 0.5, 1, 2, 4, 6 and 8 hr, 1 mL sample was withdrawn from the release medium and at the same time, the same volume of fresh mPBS was added to the receiver compartment. Using spectrophotometry, the concentrations of QCN and CRN in the receptor compartment were measured in triplicate at 252 and 426 nm, respectively.

In vitro and *ex vivo* Skin Permeation Study

While the *ex vivo* permeation study was conducted on the excised and prepared Wistar rat skin (JHAEC, Reg. No. 173/Go/Re/S/2000/CPCSEA; approved procedure No. 1641), the *in vitro* skin permeation analysis was conducted using Strat-MTM membrane. The identical Franz diffusion cell that was employed in the *in vitro* release study was utilized in this investigation too.[38,47] The prepared skin and Strat-M™ membrane were placed between donor and receiver compartments, stratum corneum towards the donor cell. The receiver compartment was then filled with 10 mL of pH 7.4 mPBS under continuous stirring at 500 rpm and maintaining a temperature of 37±2°C. 1 g of nanogel and conventional gel were evenly spread inside the donor compartment over the mounted membrane. The 1 mL sample was collected from the test solution at predetermined time intervals, *i.e.*, 0, 0.5, 1, 2, 4, 6 and 8 hr and simultaneously the same quantity of fresh mPBS was added to the receiver compartment. Using spectrophotometry, the concentrations of QCN and CRN in the receptor compartment were measured thrice at 252 and 426 nm, respectively. A figure was created by plotting the cumulative QCN and CRN diffused per membrane unit area (mg/cm^2) against time. Furthermore, Jss(µg/cm^2/h), the steady-state drug flux permeation rate, was indicated by the linear section of the graph's slope. By dividing Jss by the initial drug content in the donor compartment, the Permeability coefficient (Pcof) (cm/hr) was found. Meanwhile, the Enhancement Factor (EF) was derived by dividing nanogel Jss with conventional gel Jss.[38,47]

Dermatokinetic Study

The time-based quantification of the drug's concentration in the skin's layers is known as dermatokinetic analysis. The skin permeation study's instructions were followed for assembling this diffusion assembly. The entire skin was extracted from diffusion cell at the appropriate sample intervals of 0, 0.5, 1, 2, 4, 6 and 8 hr for this investigation. To get rid of the formulation that was stuck to the collected skin, it was repeatedly cleaned with regular saline. Following a 2 min soak in warm water heated to 50±2°C, the separation of the epidermis and dermis layers of the cleansed skin was done. The resulting solution in methanol was then passed across a 0.45 µmpore-size filter. Spectrophotometric measurements were made of the QCN (257 nm) and CRN (417 nm) contents in solution. The samples prepared identically using the dermis and epidermis of the untreated skin were taken as references. Plotting of QCN and CRN concentrations per cm^2 of skin vs time was done independently for the dermis and epidermis. Moreover, PK solver software was used for computation. Every measurement was made three times.[48]

Stability Study

In order to determine the stability of optimized nanogel, different sealed containers were stored in a dark chamber at 23±1°C for 6 months. The characteristics of nanogel were evaluated in the predetermined period (Initial, 2nd months, 4th months and 6th months) against different parameters, such as appearance, spreadability, extrudability, pH and drug content in triplicate.[43,49]

RESULTS

Compatibility Studies

First, individually and then, the mixture of QCN and CRN were visually analyzed. No color or physical changes were observed in either QCN and CRN or the mixture of them. Further, QCN and CRN and their mixture were analyzed by FTIR and DSC. The FTIR characteristic peaks of the various important functional groups were analyzed to check the mixture compatibility of QCN and CRN in its spectrum. For this purpose, the FTIR spectra of the QCN and CRN mixture were compared with the spectra of individual drugs (Figure 1a-c). There was no discernible degradation of the peaks, indicating that there was no pharmaceutical incompatibility. Figure 1 d-f depicts DSC peaks of QCN, CRN and their mixture, where with the sharp endothermic peaks for QCN and CRN, concurrently, the mixture of QCN and CRN also showed sharp peaks for both drugs. No additional peaks were observed which is an indication that no reaction between the drugs has occurred.

Selection of Lipids

The solubilities of QCN and CRN in various liquid lipids are shown in Figure 2a. It was found that QCN and CRN both showed maximum solubility in Turmeric oil; therefore, it was selected as the liquid lipid for the development of NLC formulation. The selection of solid lipids was done based on the solubility of the drug in various solid lipids as shown in Figure 2b for QCN and CRN. QCN and CRN are lipophilic drugs. Maximum solubility

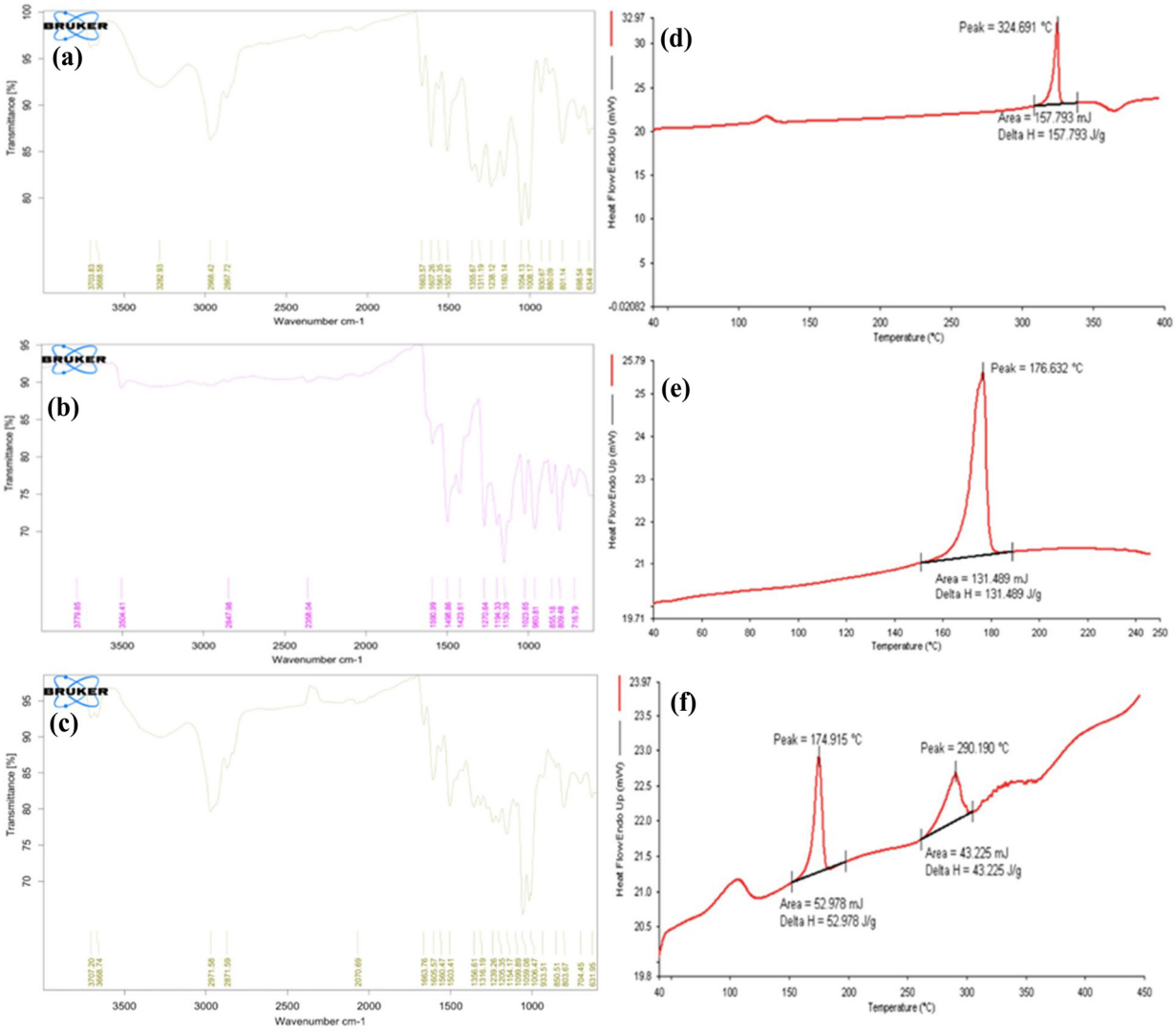

Figure 1: FTIR spectra of (a) QCN, (b) CRN and (c) mixture of QCN and CRN. DSC thermogram of (d) QCN, (e) CRN and (f) mixture of QCN and CRN.

was found in Labrafil M2130 CS, Precirol ATO 5 and Tefose 1500; therefore, they were selected as the solid lipids for further studies for the development of NLC.

Optimization of Lipid Binary Mixture

The BML having different concentrations of liquid and solid lipids were investigated where Labrafil M2130 CS and Tefose 1500 offered higher solubility for QCN and CRN, respectively, as compared to Precirol ATO 5, but they could not be selected for the formulation development due to their incompatibility with the selected liquid lipid (Turmeric oil) at room temperature. The BML of Turmeric oil+Labrafil M2130 CS and turmeric oil+Tefose 1500 exhibited clear solutions but did not solidify at room temperature, in contrast to which the BML of Turmeric oil+Precirol ATO 5 formed a clear solution and offered rapid solidification at room temperature. Hence, the mixture of Turmeric oil+Precirol ATO 5 was selected as the most suitable BML for further studies and formulation development of QC-NLC.

The best solubility levels for QCN and CRN, as well as compatibility among the chosen liquid and solid lipids, were optimized for a BML. The ideal ratio for solubilizing both medications was determined by experimenting with different solid-to-liquid lipid ratios. After smearing the two constituents on the filter paper to see if there were any liquid droplets on it, the miscibility between them was examined physically. Following this investigation, it was found that, with a solid-toliquid lipid ratio of 7:3, there were no liquid droplets on the filter paper. Additionally, it was noted that there was no evidence of component separation and that the BML (7:3) was stable.

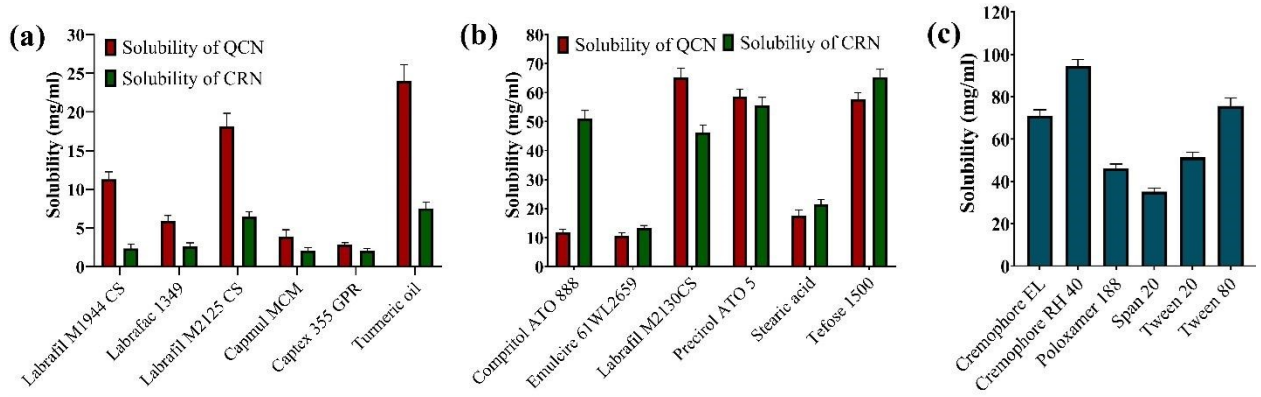

Figure 2: Selection of (a) liquid lipid, (b) solid lipid and (c) surfactant.

Table 2: CCRD experiment design and obtained responses.

Runs	Independent variables		Dependent variables			
	A: Lipid concentration (%w/v)	B: Surfactant (%w/v)	R_1: Particle size (nm)	R_2: PDI	R_3: QCT Entrapment efficiency (%)	R_4: CUR Entrapment efficiency (%)
1	2	3.5	163	0.29	90.67	96.77
2	3	2	210	0.45	92.65	96.45
3	2	3.5	154	0.29	91.62	96.18
4	3.4	3.5	198	0.55	93.12	98.32
5	0.6	3.5	99	0.12	83.91	89.35
6	3	5	179	0.45	94.57	98.90
7	1	5	96	0.13	85.16	91.68
8	2	3.5	168	0.27	91.49	96.12
9	2	3.5	168	0.28	90.48	96.54
10	2	5.6	138	0.24	89.56	94.76
11	2	1.4	193	0.30	91.13	95.52
12	2	3.5	166	0.28	90.54	97.14
13	1	2	119	0.21	86.23	93.41

Selection of Surfactant

The emulsification capability of several surfactants was screened and the results were assessed using transmittance. Figure 2c summarizes the transmittance of optimal BML (Turmeric oil:Precirol ATO5; 7:3) with different surfactants. The emulsification study's outcome showed that Cremophore® RH 40 generated an emulsion with greater transmittance (94.44±3.23%), suggesting that this surfactant emulsified BML more effectively. Consequently, the surfactant Cremophore® RH40 was chosen for the QC-NLC development.

Optimization of Combinatorial Nanostructured Lipid Carrier (QC-NLC) Using CCRD

CCRD was applied to optimize and select a combinatorial QC-NLC formulation. Thirteen runs in total were recommended by the design expert® software and these were designed and assessed to find out how BML and surfactant concentrations affected particle size, PDI and %EE. Table 2 tabulates the response that was observed. Using ANOVA, the model's significance was ascertained. At a 95% confidence level, quadratic polynomial models with big F-values and modest *p*-values show significant relevance. The findings demonstrated an excellent fit to the proposed models and that the model terms were highly important in relation to each of the four responses. The link between the expected and actual values for the dependent variables, as well as 3D response surface plots and contour plots, were created to illustrate the interaction between the independent factors and responses, as seen in Figure 3. Several statistical mathematical metrics, including multiple correlation coefficients (R^2) and modified multiple correlation coefficients (R^2), were compared to determine which mathematical model fit the data the best. The model's fitness was confirmed by the non-significant *p*-value for lack of fit, which showed a few pure mistakes.

Outcomes of the Independent Factor on Particle Size

ANOVA analysis of CCRD provided a quadratic model that was found to be significant ($p<0.0001$) with a F-value of 49.85, indicating that the model was significant after the data was interpreted in the various models. The likelihood of noise producing an F-value greater than this is merely 0.01%. Models are treated as significant when *p*-values are <0.05. A, B and A^2 are found important in this instance. There was a decent degree of agreement between the adjusted R^2 value (0.95) and the projected R^2 value (0.85), as evidenced by the difference being less than 0.2. The interaction term in a quadratic model represents the combined effect of two variables and can have a positive or negative impact on quality criteria. In this instance, significant ($p<0.05$) model terms included A (BML) and B (surfactant), where AB was predicted using the following equation:

Particle size=+163.80+39.25A-16.47B-2.00AB-9.15A2-0.65B2

The contrary outcome of independent variables on particle size was revealed by the equation's interaction term AB (-2.0) and the negative coefficient of variable B (-16.47). Variable A's considerable coefficient number suggested that it had a greater impact on particle size than variable B. Additionally, factor A's positive coefficient (+39.25) suggested that it had a favorable impact on particle size. It was concluded from response surface plots that particle size was considerably impacted by BML and surfactant concentration (Figure 3a, e and i). The plot of the predicted and actual values is reported in Figure 3e. The outcome of independent factors like concentration of BML and surfactant concentration revealed that particle size of formulations hiked with an increase in concentration of BML, whereas it fell short with increasing surfactant concentration after fitting the data of response in the model.

Outcomes of the Independent Factor on PDI

Among all the parameters of the formulation process, PDI is also a crucial parameter which reflects the uniform dispersion and physical stability of nanoparticles in NLCs. To maintain stability over the long run, values must be as low as feasible. A desired homogenous nanoparticle distribution is indicated by PDI values <0.3, whereas an extremely wide range of PDI values greater than 0.5, representing heterogenicity of nanoparticle distribution.[50] The results of the experiment were examined and the quadratic model was found to be highly significant ($p<0.001$), according to ANOVA analysis. Model F-value of 328.12 suggested that the model was significant. The predicted R^2 of 0.98 was in suitable agreement with the adjusted R^2 of 0.99 because the difference between them was less than 0.2. The software suggested the quadratic equation below to describe the effects of the terms on PDI.

$$PDI=+0.28+0.15A-0.02B+0.02AB+0.03A^2-0.005B^2$$

The negative coefficient variables B (-0.02) and B2 (-0.005) indicated a negative effect on the PDI, while other coefficient variables were the positive variables that had a positive effect on the PDI (Figure 3b and j). The effect of surfactant and BML concentration was studied on PDI. PDI is not significantly impacted by increasing the concentration of surfactants in the systems. However, the particles with very smaller sizes may sometimes coalesce to form larger particles, which may disturb the uniformity of distribution of the nanoparticles and may increase the value of PDI for that system.

Outcomes of the Independent Factor on Entrapment Efficiency

The range of 83.91 to 94.57% was found for EE for QCN of the 13 formulations that were obtained. It is a crucial parameter that affects formulation since it controls how the drug is delivered at the right dose for the therapeutic efficacy that is included in NLC. Thus, research was done on how BML and surfactant

concentration affected this attribute feature. The quadratic model was used to fit the repose data. The model was deemed significant ($p<0.0001$) based on its F-value of 46.86. The predicted R^2 of 0.85 was in decent agreement with the adjusted R^2 of 0.95. The lack of fit Fvalue of 2.50 suggested the fact that the lack of fit couldn't be considered significant compared to error. The following equation describes the effect of terms on EE.

$$\text{Entrapment efficiency} = +90.96 + 3.61A - 0.17B + 0.75AB - 1.17A^2 - 0.26B^2$$

The coefficient variable of -0.17 for B showed its adverse effect on the EE. The positive value of variable A (+3.61) and interaction variable AB (+0.75) had a positive effect on the EE (Figure 3c and k). It also investigated how the independent variable affected the CRN's EE. The quadratic model was used to fit the response data from the EE. The model was significant ($p<0.0001$), as evidenced by the model F-value of 43.27. The difference between the adjusted R^2 of 0.95 and the expected R^2 of 0.82 was less than 0.2, indicating reasonable agreement. The F-value for lack of fit,

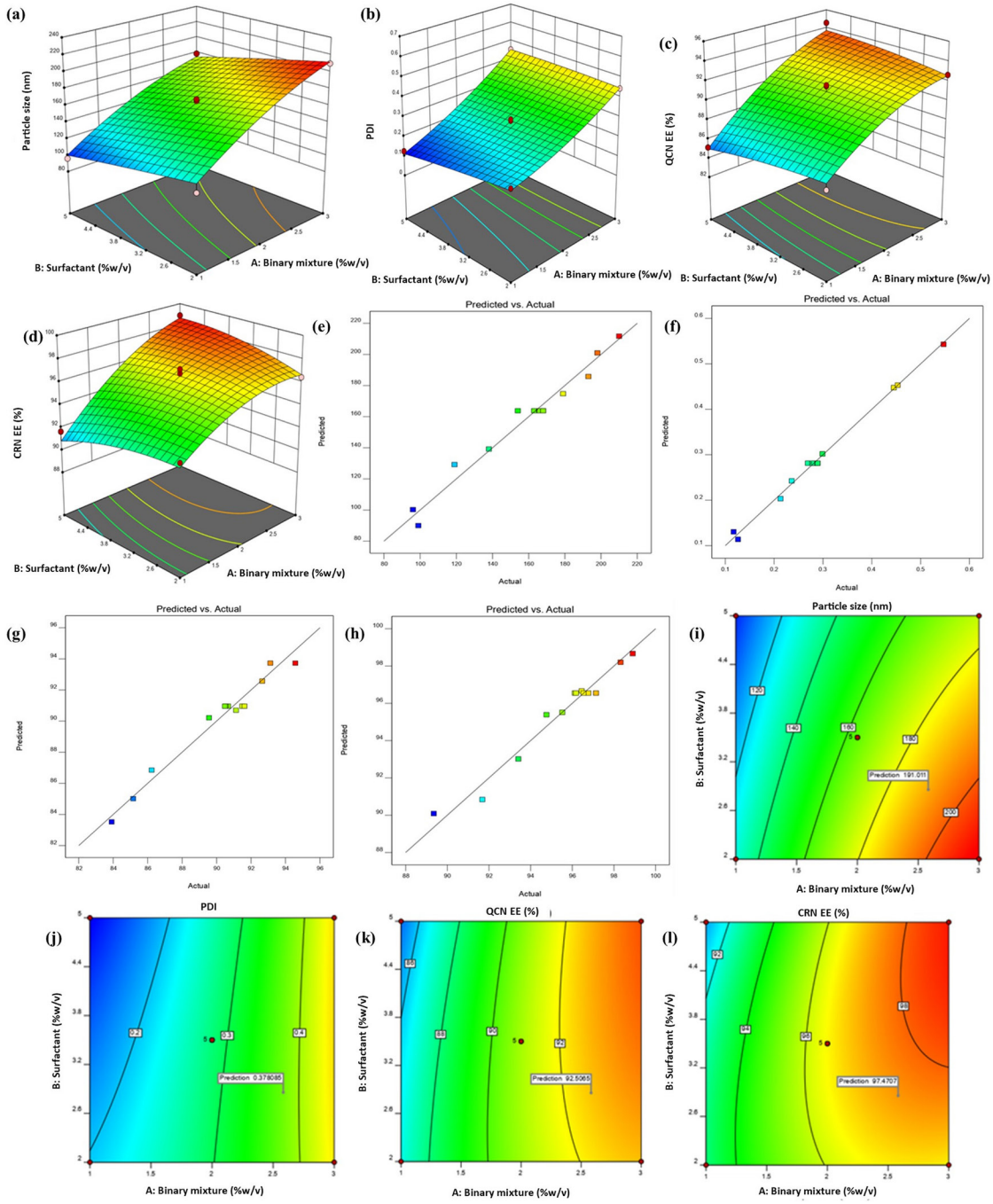

Figure 3: Effect-responses plots effect determination of binary mixture and surfactant on (a) particle size, (b) PDI, (c) %EE of QCN, (d) %EE of CRN; predicted vs actual values graph of (e) particle size, (f) PDI, (g) EE of QCN, (h) EE of CRN; contour plot of (i) particle size, (j) PDI, (k) EE of QCN and (l) EE of CRN.

which was 3.55, suggested that the lack of fit did not significantly affect the error. Model fit was indicated by a negligible lack of fit. The following is the quadratic equation that the program suggests be used to explain how terms affect the EE of a CRN.

$$\text{Entrapment efficiency} = 96.55 + 2.87A - 0.04B + 1.05AB - 1.20A2 - 0.55B^2$$

p-values <0.05 declared model terms are statistically significant. The coefficient variable B harmed the EE, but variable A was a significant model term that had an upright effect on the EE. The impact of the independent variable on the EE was analyzed and it was concluded that an increase in the concentration of BML results in an increase in EE, whereas a high surfactant concentration results in a slight decrease in EE (Figure 3d and l).

Optimization and Formulation of Optimized QC-NLC

Software-based results analysis of all the runs provided an optimized formula for the development of a combinatorial QC-NLC containing 2.0% w/v lipid and 3.5% w/v surfactant. The mean size of the particle and PDI of optimized QC- NLC was recorded as 163.8±1.5 nm and 0.28±0.04, respectively. Next, the surface charge of the developed QC-NLC was recorded, which was found to be -31.6±1.4 mV, which comes in the range of stable systems, and it showed system stability due to the repulsion between the charges.

Study of Surface Morphology

TEM analysis was executed to determine the surface structure of optimized QC-NLC (Figure 4). Figure 4 exhibited a dark-colored core of QC-NLC, where the darkness of the core indicated the presence of drugs in the lipids. The figure showed nanoparticles of size <200 nm, which is an optimum size for the delivery of particles across the stratum corneum.

Appearance, Drug Content and pH of Gel Formulations

The prepared combinatorial nanogel and conventional gel formulation of QCN and CRN characterization were done in terms of appearance, percent drug content and pH. Both gel formulations were found to be dark yellow translucent semisolid masses with a gel-like consistency. The pH of nanogel and conventional gel was recorded as 6.93±0.59 and 6.60±0.46, respectively and both gel formulations exhibited a smooth homogenous characteristic. Additionally, nanogel contained 91.10±2.38% QCN and 96.24±1.90% CRN and conventional gel carried 97.89±4.84% QCN and 98.24±4.35% CRN.

Spreadability and Extrudability of Gel Formulations

The spreadability of nanogel and conventional gel were found to be 6.23±0.40 cm and 6.09±0.43 cm. The spreadability of nanogel was found to be negligibly higher than conventional gel. It may be due to BML, which may have reduced the friction between the applied surface and formulations. Moreover, the obtained values for all gels indicated good spreadability. The extrudability of nanogel and conventional gel of QCN and CRN was recorded as 40.33±2.08 g/cm^2 and 60.33±1.53 g/cm^2, respectively. Extrudability is shear stress corresponding to a shear rate exceeding yield stress so that formulation starts to flow. Application of a smaller value of force to extrude the gel out of the tube is usually an indication of a good quality gel, whereas higher forces would be required to extrude the gel whose quality has been compromised. Higher forces were required to extrude the conventional gel from the tube in comparison to the nanogel. So, the nanogel has less value of extrudability which offers an advantage over the conventional gel.

Occlusive Efficacy

Moreover, an occlusive efficacy study of gel formulations was performed to check their soothing efficacy because in diseased conditions and due to different factors, skin becomes damaged and dry. In this study, Vaseline was used as a control in order to compare the occlusive effect of QCNLC-based nanogel. After 48 hr, the occlusion factors of the control, nanogel and traditional gel were, respectively, 87.65%, 73.49% and 25.98±2.89% (Figure 5a). The result revealed that Vaseline clearly represented the highest occlusion factor. The occlusion factor for nanogel showed significantly (p<0.0001) better than conventional gel, while the occlusion factor for nanogel showed significantly (p<0.008) lower compared to the control.

Texture Analysis

The texture characteristics of both the nanogel and conventional gel were performed through analysis of force-time plot which provides information on parameters like hardness, adhesiveness and cohesiveness of the gel. The cohesiveness, adhesiveness and hardness of the gels are represented by the maximum force and work done to deform the gel in the down speed of the probe

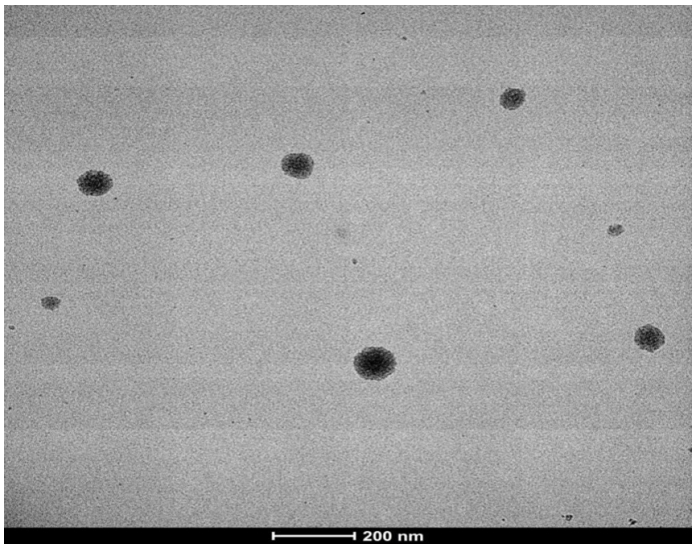

Figure 4: TEM image of optimized combinatorial QC-NLC.

and the second area of the curve, respectively.[51] The values of consistency, cohesiveness, hardness and viscosity index were 287.45 g.sec, 157.09 g, 206.56 g and 259.87 g.sec, respectively, for QC-NLC nanogel and 101.13 g.sec, 57.44 g, 120.05 g and 65.17 g.sec, for conventional gel.

In vitro Drug Release from Gel Formulations

Figure 5b shows the release profiles of QC-NLC-based nanogel and conventional gel at 7.4 pH. These results interpreted that lipid carriers can control drug release in the used medium, where 93.26±3.76% QCN and 97.13±3.08% CRN were released from nanogel after the completion of the release study. In contrast, conventional gel only released 53.95±2.48% QCN and 58.17±2.51% CRN. In mPBS media, QCN and CRN exhibited an initial burst release till 60 min from the nanogel and further, it showed a prolonged release till 8 hr.

In vitro and *ex vivo* Permeation Screening

In vitro and *ex vivo* permeation analysis of nanogel and conventional gel were executed using Strat-M™ membrane and mice skin, respectively and a correlation between *in vitro* and *ex vivo* permeation of the drug was established. *In vitro* permeation profile of QCN in nanogel and conventional gel showed 261.23±6.22 μg/cm^2 and 119.15±3.60 μg/cm^2 permeation, whereas the *ex vivo* permeation exhibited 257.71±3.83 μg/cm^2 and 117.56±3.05 μg/cm^2 over 8 hr of experiment, respectively (Figure 6a and b). Simultaneously, *in vitro* permeation of CRN in nanogel and conventional gel showed 287.80±7.46 μg/cm^2 and 133.46±4.68 μg/cm^2 permeation, whereas the *ex vivo* experiments exhibited 298.25±6.52 μg/cm^2 and 132.47±4.99 μg/cm^2 permeation over 8 hr of experiment, respectively (Figure 6a and b). Additionally, flux and permeation coefficients were also determined for each drug and every formulation. *In vitro* flux of QCN of nanogel and conventional gel showed 24.61±0.45 μg/cm^2/hr and 12.26±0.42 μg/cm^2/hr, whereas the *ex vivo* flux exhibited 24.28±0.34 μg/cm^2/hr and 11.84±0.23 μg/cm^2/hr, respectively. Simultaneously, *in vitro* flux of QCN of nanogel and conventional gel showed 26.99±0.68 μg/cm^2/hr and 13.05±0.63 μg/cm^2/hr, whereas the *ex vivo* flux exhibited 27.93±1.46 μg/cm^2/hr and 13.16±0.50 μg/cm^2/hr, respectively.

Additionally, the *in vitro* permeation coefficient of QCN of nanogel and conventional gel showed 0.062±0.001 cm/hr and 0.031±0.001 cm/hr, whereas the *ex vivo* flux exhibited 0.061±0.001 cm/hr and 0.030±0.001 cm/hr, respectively. Simultaneously, *in vitro* permeation coefficient of QCN of nanogel and conventional gel showed 0.034±0.001 cm/hr and 0.016±0.001 cm/hr, whereas the *ex vivo* flux exhibited 0.035±0.002 cm/hr and 0.016±0.001 cm/hr, respectively.

Screening of Dermatokinetic Behavior

In the dermatokinetic screening, the epidermal and dermal concentrations of QCN and CRN are described in Figure 7, which shows maximized QCN and CRN deposition at the layers of skin from nanogel rather than conventional gel. Simultaneously, from the obtained data, the $AUC_{0\text{-}8h,}$

$C_{skin\text{-}max}$ and $T_{skin\text{-}max}$ of QCN and CRN in layers of skin were also calculated. $C_{skin\text{-}max}$, $T_{skin\text{-}max}$ and $AUC_{0\text{-}8h}$ of QCN and CRN of nanogel in epidermis were recorded as 203.81±4.56 μg/cm^2, 418.41±29.07 μg/cm^2, 1.17±0.76 hr, 1.17±0.76 hr, 1400.59±52.23 μg.cm^{-2}hr and 2672.04±44.36 μg.cm^{-2}hr. Whereas, in the dermis $C_{skin\text{-}max}$, $T_{skin\text{-}max}$ and $AUC_{0\text{-}8h}$ of QCN and CRN of nanogel were observed as 212.54±4.70 μg/cm^2, 400.81±14.39 μg/cm^2, 0.83±0.29 hr, 0.83±0.29 hr, 1468.08±4.52 μg.cm^{-2}h and 2677.95±56.81 μg.cm^{-2}h. $C_{skin\text{-}max}$, $T_{skin\text{-}max}$ and $AUC_{0\text{-}8h}$ of QCN and CRN of conventional gel in the epidermis were recorded as 107.29±4.56 μg/cm^2, 207.99±8.51 μg/cm^2, 0.67±0.29 hr, 0.83±0.29 hr, 678.13±51.17 μg.cm^{-2}hr and 1314.72±87.93 μg.cm^{-2}hr.

Whereas, in the dermis $C_{skin\text{-}max}$, $T_{skin\text{-}max}$ and $AUC_{0\text{-}8h}$ of QCN and CRN of conventional gel were observed as 118.35±9.90 μg/cm^2, 219.87±7.53 μg/cm^2, 0.83±0.29 hr, 0.83±0.29 hr, 754.85±64.79 μg.cm^{-2}hr and 1450.27±93.55 μg.cm^{-2}hr.

Stability Studies

To check the storage ability of developed nanogel stability studies were carried out. Firstly, the appearance of optimized nanogel was

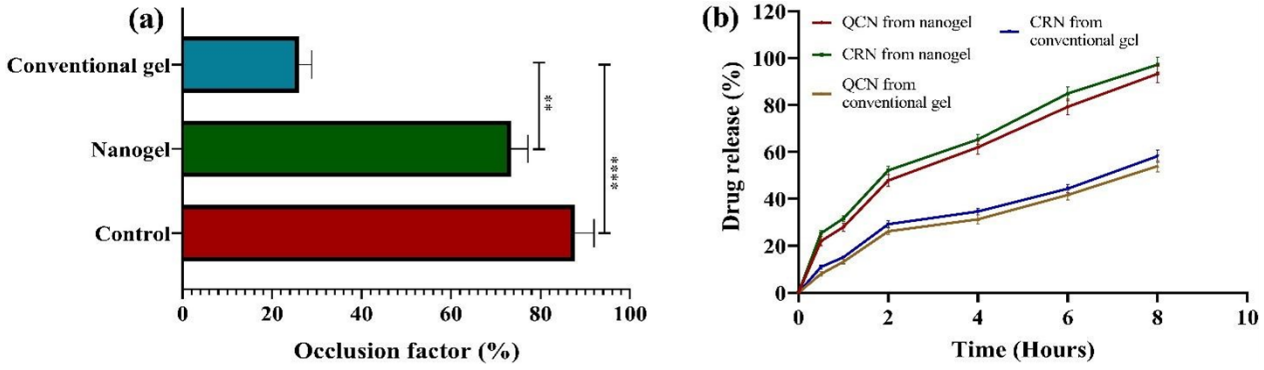

Figure 5: (a) Occlusion efficacy of combinatorial nanogel and conventional gel in comparison to Vaseline (control). Statistical comparison: ****p<0.0001 vs. conventional gel, **p<0.01 vs. control and (b) release profiles of QCN and CRN from the nanogel and conventional gel at pH 7.4.

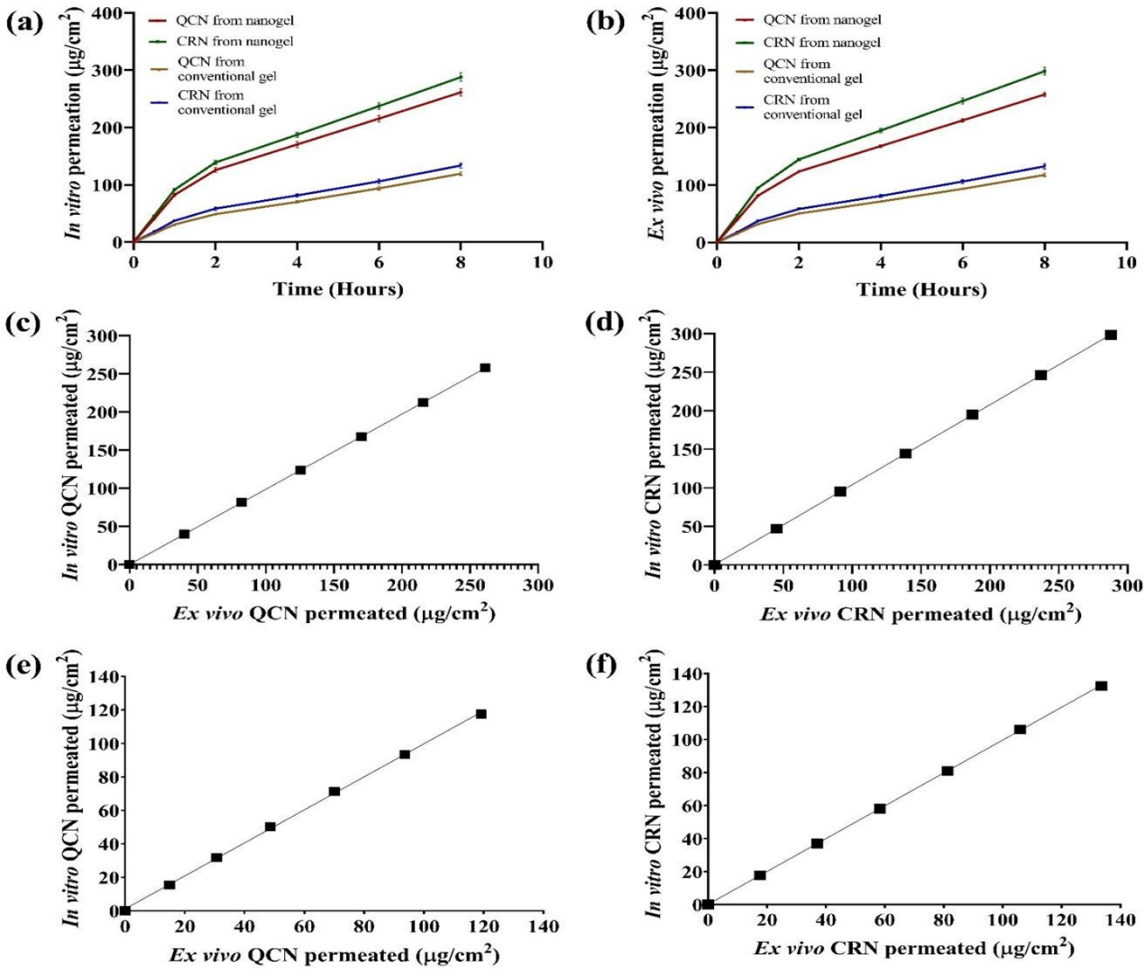

Figure 6: (a) *In vitro* permeation plot of QCN and CRN of nanogel and conventional gel, (b) *Ex vivo* permeation plot of QCN and CRN of nanogel and conventional gel, (c) and (d) a linear relationship between *in vitro* and *ex vivo* QCN and CRN permeation from nanogel, (e) and (f) a linear relationship between *in vitro* and *ex vivo* QCN and CRN permeation from the conventional gel.

evaluated and no notable changes were observed. Concurrently, extrudability, spreadability, pH and drug content of nanogel were evaluated and also statistically analyzed, which showed the insignificant difference between the Initial and 6thmonth samples. Thus, the results of the studies showed the surpassing storage ability of nanogel (Figure 8).

DISCUSSION

This research work was performed with the scope of development of a novel QC-NLC based gel formulation for the management of skin cancer through the CCRD by using Design expert® software. Before the initiation of formulation development, the first compatibility study was executed. The drug-drug compatibility study is a fateful parameter to determine any physical change and the structural modifications between the two drugs and to ensure that both drugs do not affect the stability of each other. QCN is a yellow crystalline solid, whereas CRN is found as an orange-yellow crystalline solid powder and after mixing, no color or physical changes were recorded in the samples. For further confirmation, FTIR and DSC analyses were performed. The FTIR spectra displayed distinctive peaks at positions but with minor shifting in a few peaks. Therefore, it was verified that there were no structural changes when the two drugs were combined because a mixture of QCN and CRN contained all of the distinctive peaks (Figure 1 a-c).

DSC analysis was also performed to avoid the possibility of incompatibilities between these two drugs. DSC peaks of QCN and CRN and their mixture demonstrated sharp endothermic peaks (Figure 1 d-f). No additional peaks were observed which is an indication that no reaction between the drugs has occurred.

During the selection of liquid lipids, turmeric oils were selected based on the maximum solubility of QCN and CRN in it. Turmeric oil is a rich source of curcuminoids and is expected to enhance the anticancer potential of our selected compounds. Additionally, turmeric oil and CRN share the same source of origin, *i.e.*, they are the essential oil and curcuminoid obtained from *Curcuma longa* L. Therefore, it was anticipated that the selection of this oil for formulation development would augment the anticancer potential of selected compounds. Whereas Labrafil M2130 CS, Precirol ATO 5 and Tefose 1500 were picked as solid

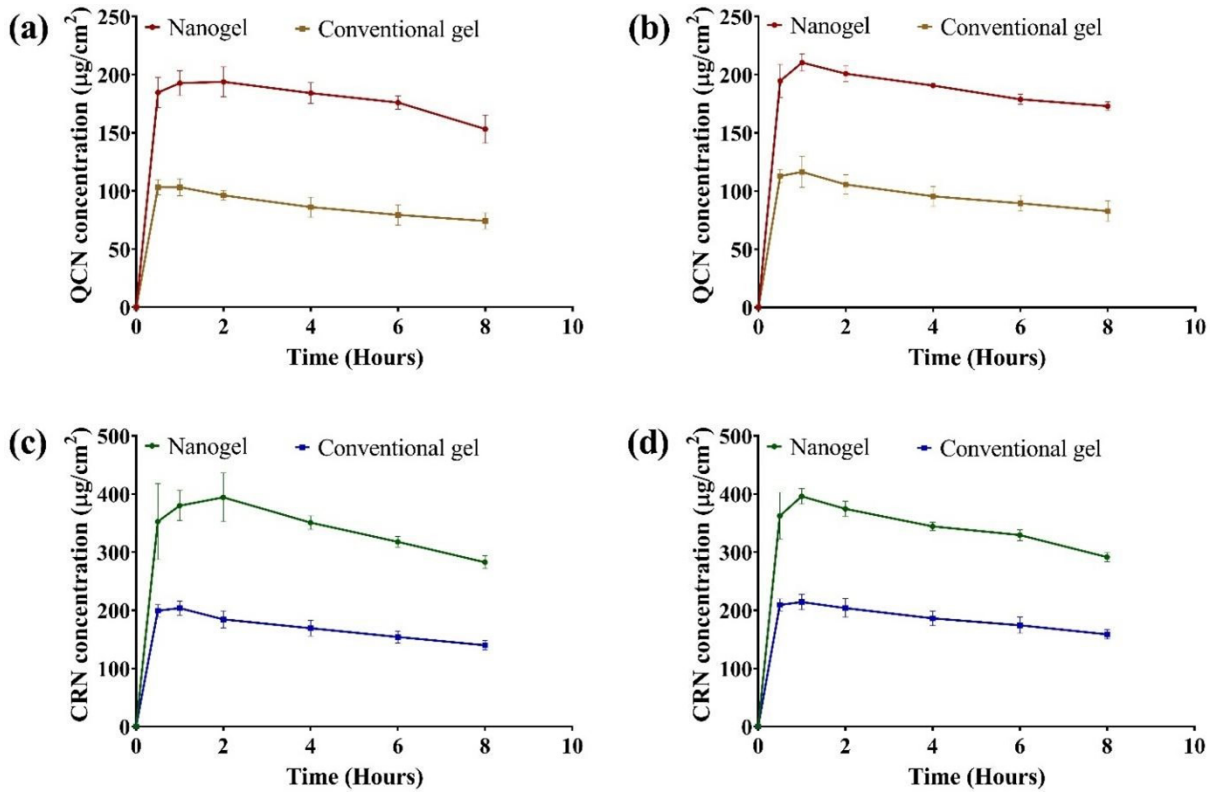

Figure 7: Comparative dermatokinetic profile depicting the drug concentrations (a) QCN in the epidermis, (b) QCN in the dermis, (c) CRN in the epidermis and (d) CRN in the dermis.

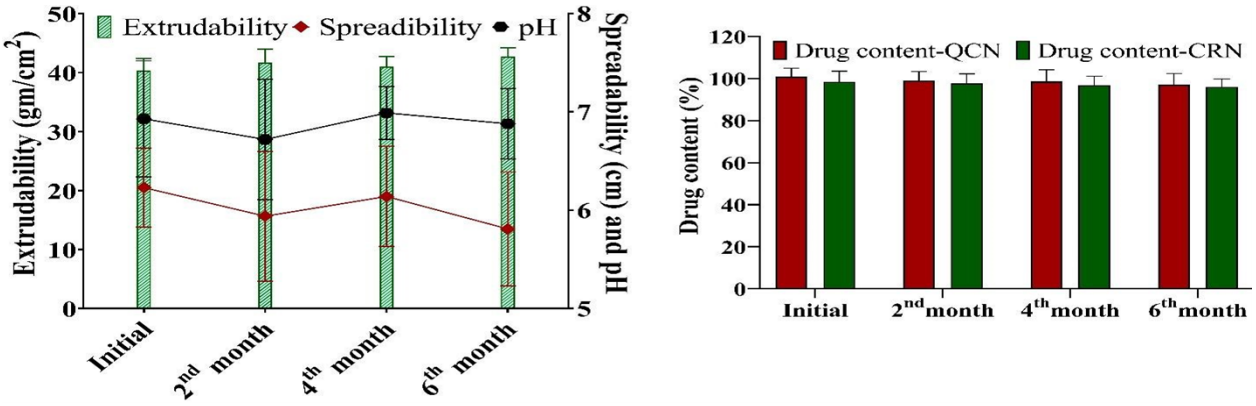

Figure 8: Results of stability studies.

lipids based on the maximum solubility of QCN and CRN in them for further studies of NLC development. From the selected solid lipids, Precirol ATO 5 was chosen as the most suitable solid lipid because it gave the most stable BML with turmeric oil compared to Labrafil M2130 CS and Tefose 1500. Further, a solid-to-liquid lipid ratio study was performed and a 7:3 ratio was selected as the best ratio based on the complete mixing of oil in the solid lipid. As is known, one important excipient used in NLC formulations is surfactant. So, the selection of surfactant was performed based on the maximum solubilizing capacity of lipid. In this case, the transmittance of a liquid solution was recorded and the surfactant and lipid solution showing the maximum transmittance was selected as a surfactant. Research has been done on the application of several non-ionic surfactants in the creation of NLC. Furthermore, the formulation's toxicity, crystallinity and physical stability may be affected by their concentration and composition.[52] Cremophore® RH 40 showed maximum transmittance, so it was selected as a surfactant for NLC development. Cremophore® RH40, one type of non-ionic surfactant, is a polyoxy 40 hydrogenated castor oil. When used in a formulation for topical use, it can function as a surfactant, emollient, solubilizer and permeation enhancer. It is classified as Generally Recognized as Safe (GRAS) and is non-toxic.

Since NLC is a novel and stable lipid-based nanocarrier compared to others, it is a preferred nanocarrier among scientists for topical applications. NLC improves the bioavailability of

drug molecules across the skin layers in various ways, such as by inhibiting the degradation of drugs through their encapsulation and by increasing permeation through its nanosized particles. Because particle size affects both the rate of permeation and the amount of drug disposition in the skin, it is one of the most crucial quality characteristics in the manufacture of NLC formulation. Particle sizes smaller than 200 nm were preferred for topical application.[53,54] NLC also exhibits sustained release of drugs. So, in the present work, NLC was selected as a remarkable nanocarrier for greater anti-skin cancer efficacy through the improved bioavailability of QCN and CRN in diseased areas. Because BML concentration and surfactant have a direct impact on the particle size, PDI and EE, where a high concentration of BML increases the particle size, PDI and EE and an increased concentration of surfactant reduces it due to its interfacial force reduction properties. So, optimization of the required concentration of BML and surfactant were critical variables and it was performed through experimental design software. Response Surface Methodology (RSM) is a potent statistical technique that works well in multivariate analysis to examine the connections between response and independent variables. By establishing the ideal parameters, it is simple to optimize some processes using mathematical concepts. Additionally, the bare minimum of trial runs is carried out in order to thoroughly evaluate the impact of independent factors and the ways in which they interact with one another on the chosen replies.[55] CCRD was applied to optimize the combinatorial QCN and CRN-loaded NLC, which is the most acceptable optimization tool in the development of optimized drug formulation as it enables accurate forecasts across a broad variety of variables and at extreme levels of variation. These techniques save money and time because they involve a very small number of experiments. A total of thirteen runs were obtained from the software design and the results of all runs were analyzed in the software. After a full analysis, a formulation comprising lipid (2.0% w/v) and surfactant (3.5% w/v) was picked as an optimized nanoformulation because it had the desirability factor 1. It also fulfilled the criterion for optimal performance. Having generated the polynomial equation relating to the four responses and in order to find the best compromise between them, the desirability function was used. The optimized formulation was prepared and evaluated for particle size, PDI, and surface charge. The NLC formulation was optimized concerning its BML. The mean size of the particle and PDI of optimized combinatorial QCN and CRN-loaded NLC were found to be 163.8±1.5 nm and 0.28±0.04, respectively. The size distribution and uniformity of dispersion are indicated by the PDI. The PDI of a homogeneous monodisperse system ought to be near 0.0. A wide polydispersity system is indicated by a PDI greater than 0.4. Moreover, a PDI score ranging from 0.10 to 0.40 indicates a substantial polydisperse system. The distribution of particles in a system with moderate polydispersity is neither wide nor narrow.[56]

By measuring particle charge and electrostatic repulsion, zeta potential is a metric for evaluating the physical stability of colloidal dispersions. Ionization of surface groups or ion adsorption causes the surfaces of particles to become charged. The media around the particles, as well as the surface chemistry of the particles, affect this charge.[57] The surface charge of the developed QC-NLC was found to be -31.6±1.4 mV, which comes in the range of stable systems and it showed system stability due to the repulsion between the charges. The recorded zeta potential is due to both surfactant and BML. As it is known, the zeta potential within the range of -30 to +30 mV is considered stable. Systems having zeta potential within the range of -60 to +60 mV are recognized to have excellent stability as the more positive or negative values of surface potential increase the repulsion between the nanoparticles, thus decreasing the chances of agglomeration and enhancing the stability of the nanosystem.[58,59] Thus, the surface potential of the formulation showed that the developed system was highly stable due to the repulsion between the particles. The EE was also calculated, which provided more than 90% entrapment of QCN and CRN in developed optimized QC-NLC and the high EE was due to the solubility of QCN and CRN in turmeric oil and Precirol ATO5. Figure 4 showed spherical nanoparticles of size <200 nm. The obtained particle size was desired for the permeation of the drug across the stratum corneum because a particle size less than 200 nm would permeate all the skin layers and carry the possibility of reaching the systemic circulation, which depicts the failure of the developed NLC system, whose aim was to deposit the drugs into the skin layers.[60]

After the characterization of optimized QC-NLC, its gel formulation was developed using Carbopol 934. Combinatorial nanogel was found as dark yellow translucent semisolid masses with a gel-like semisolid consistency. Spreadability is an important quality parameter of topical formulations such as creams, ointment, gel, etc., from the perspective of a patient. The comparative spreadability and extrudability of nanogel were carried out with conventional gel and the results of studies exhibited favorable outcomes for nanogel. The reasons behind the results were the presence of Turmeric oil and Precirol ATO5 in the nanogel, which provided smooth flow and spreadabilty of nanogel formulation. The stratum corneum normally maintains a 10-25% hydration state in the skin. However, exposure to pollutants such as solvents, UV radiation, etc., injury and some dermatological conditions may damage the stratum corneum. The skin may become dry as a result of TEWL after stratum corneum rupture. As a result, topical formulations used to treat skin disorders should have high occlusive characteristics to maintain the water in the skin. TWEL is one of the major issues with numerous skin conditions. So, in the occlusive efficacy study, the effectiveness of gel formulations was analyzed and compared with Vaseline, which was used as a control. After 48 hr of study, the occlusion factor for nanogel showed better than conventional gel, while the occlusion factor for nanogel was recorded lower compared to the

control. Hence, results showed that the gel containing lipid-based nanocarrier had a significantly higher occlusion factor than the gel without lipid carrier because lipids of formulation create a thin film, which prevented excessive TEWL and it is also confirmed by a previous study.[43]

In vitro drug release study described a prolonged release of QCN and CRN from nanogel after the initial burst release of drugs. These characteristics can be ascribed to the presence of drugs at the superficial layer and then the liberation of QCN and CRN from the inner core of NLC. QCN and CRN were then released constantly until the saturation point. In addition, the release of drugs was found less from conventional gel than nanogel, showing its size and permeability dependency. These results can be attributed to the characteristics of the release profile and are substantiated by similar findings.[38] The release was lower from conventional gel due to the uneven particle size, leading to a decrease in the permeation ability of the drug molecules. These outcomes are needed for forecasting the possible release of QCN and CRN after topical application. Thus, the drug can be retained on the infected area through the nanogel for a prolonged time to deliver high amounts of QCN and CRN to the target tumor site. *In vitro* and *ex vivo* permeation analysis exhibited significantly higher ($p<0.05$) for QCN and CRN permeated from nanogel compared to drugs permeated from the conventional gel. The higher rate of permeation profile of QCN and CRN of nanogel than conventional gel could be due to nanosized particles, which led to more permeability of drugs through wide surface area and improved particle-skin binding. Simultaneously, the surfactants and lipids could also modify the stratum corneum of the skin through its disruption, leading to skin hydration, which in turn improved permeation. A linear permeation relationship was found when comparing the *in vitro* data against *ex vivo* permeation data of QCN and CRN of nanogel and conventional gel (Figure 6). The obtained R^2 value near one recommended a close association between *in vitro* and *ex vivo* experiments performed.

The paramount downside of the conventional drug delivery system, especially one that has herbal active ingredients, carries bioavailability issues in which solubility and permeation of drug molecules are restricted after topical application. That's why nano-based herbal drug delivery is a choice of drug delivery system for a group of scientists, which executes effective delivery of drug molecules in diseased areas.[16,61] Therefore, the deposition of drug molecules from nanogel and conventional gel in the skin layers was scanned at different intervals of time and the QCN and CRN concentrations were quantified in the epidermis and dermis of the skin under dermatokinetic screening. 1.8 times more QCN $C_{skin\text{-}max}$ of nanogel was found than the QCN $C_{skin\text{-}max}$ of conventional gel in the epidermis and dermis layer. Whereas the CRN $C_{skin\text{-}max}$ of nanogel was found to be 2 times more than the CRN $C_{skin\text{-}max}$ of conventional gel in the epidermis. On the other hand, the CRN $C_{skin\text{-}max}$ of nanogel was recorded 1.8 times more than the CRN $C_{skin\text{-}max}$ of conventional gel in the dermis layer. Similarly, $AUC_{0\text{-}8\ hr}$ of QCN of nanogel was found to be 2 times higher than the $AUC_{0\text{-}8h}$ of QCN of conventional gel in the epidermis and dermis layer. The $AUC_{0\text{-}8h}$ of CRN of nanogel was found to be 2 times higher than the $AUC_{0\text{-}8\ hr}$ of CRN of conventional gel in the epidermal layer, whereas the $AUC_{0\text{-}8h}$ of CRN of nanogel was recorded to be 1.8 times higher than the $AUC_{0\text{-}8\ hr}$ of CRN of conventional gel in the dermal layer (Figure 7). Hence, nanogel exhibited more prominent dermatokinetic behavior than the conventional gel. The results of drug release, skin penetration and dermatokinetic behavior of the nanogel corroborate each other. Overall, the QC-NLC-based nanogels demonstrated sustained release of QCN and CRN from the nanogel matrix, providing prolonged and maximum bioavailability in the diseased area. Ultimately, this will enable improved anti-skin cancer efficacy of the drug molecules. Furthermore, stability studies were performed where insignificant differences were observed between initial and 6th month samples of nanogel, which indicated its surpassing storage efficiency.

CONCLUSION

In the current studies, preformulation studies were performed after the compatibility issue between QCN and CRN was satisfied. Then, CCRD was used for combinatorial NLC development and an optimized formula was obtained. After that combinatorial NLC-based nanogel and a combinatorial conventional gel of QCN and CRN were prepared and evaluated. Nanogel possessed significantly better ($p<0.05$) occlusion behavior and release profile than conventional gel. The permeation and dermatokinetic studies showed higher flux and drug distribution ability in the layers of skin. Further, depth analysis revealed a higher availability of drug molecules when nanogel was topically applied. Stability studies of nanogel showed its surpassing storage ability. In conclusion, studies confirmed that the topically applied nanogel could be a potential approach for skin cancer treatment due to appreciably improved bioavailability in the layers of skin.

ACKNOWLEDGEMENT

This work is dedicated to Late Sadaf Saleem.

FUNDING

The Deanship of Scientific Research (DSR) at King Abdulaziz University (KAU), Jeddah, Saudi Arabia has funded this project under grant no (KEP-MSc:14-166-1443).

CONFLICT OF INTEREST

The authors declare that there is no conflict of interest.

ABBREVIATIONS

QCN: Quercetin; **CRN:** Curcumin; **NLC:** Nanostructured lipid carriers; **QC-NLC:** QCN and CRNloaded combinatorial NLC; **CCRD:** Central composite rotatable design; **NMSC:** Nonmelanoma skin cancer; **BCC:** Basal cell carcinoma; **SCC:** Squamous cell carcinoma; **WHO:** World Health Organization; **TEWL:** Transepidermal water loss; **DSC:** Differential scanning calorimetry; **FTIR:** Fourier Transform Infrared Spectroscopy; **BML:** Binary mixture of lipid; **PDI:** Polydispersity index, **EE:** Entrapment efficiency; **ANOVA:** Analysis of variance; **nm:** Nanometer; **TEM:** Transmission electron microscopy; **P_{cof}:** Permeability coefficient; **EF:** Enhancement factor; **J_{ss}:** Steady-state flux; **GRAS:** Generally recognized as safe; **RSM:** Response surface methodology; **mPBS:** Methanolic phosphate buffer solution; **NF-κB:** Nuclear factor kappa-light-chain-enhancer of activated B cells; **COX-2:** Cyclooxygenase-2, **PCNA:** Proliferating cell nuclear antigen; **EGFR:** Epidermal growth factor receptor; **Akt:** Protein kinase B; **Notch-1:** Neurogenic locus notch homolog protein 1; **Hif-1:** Hypoxia inducible Factor-1; **p53:** Tumor protein; **PPAR-α:** Peroxisome proliferator-activated receptor alpha; **Nrf2:** Nuclear factor erythroid-2-related factor 2; **CDKs:** Cyclin-dependent kinases; **VEGF:** Vascular endothelial growth factor; **MMPs:** Matrix metalloproteinases; **HDAC:** Histone deacetylase.

SUMMARY

A dual drug-loaded combinatorial NLC of QCN and CRN was developed through the CCRD response surface design to improve the bioavailability of QCN and CRN in skin cancer treatment.

Where first compatibility studies between QCN and CRN were performed, which showed compatibility between them. Various QC-NLCs were prepared according to runs obtained from the CCRD design. Lipid and surfactant concentration were used as independent variables and mean particle size, PDI and EE were considered as responses where the impact of independent variables was analyzed over responses. After a full analysis, a formulation comprising lipid 2.0% w/v and surfactant 3.5% w/v was selected as an optimized formula because it had the desirability factor 1. Furthermore, optimized QC-NLC was converted into a gel formulation where carbopol 934 was used as a gelling agent and the gel was neutralized with triethanolamine. Nanogel was characterized by different parameters such as appearance, drug content, pH, spreadability, extrudability, occlusiveness and texture of gel formulations. QC-NLC gel exhibited sufficient enough spreadability and low extrudability compared to conventional gel. The occlusion factor for nanogel showed significantly better results than conventional gel. *In vitro* release, permeation and dermatokinetic studies demonstrated favorable results for nanogel compared to conventional gel. Stability studies showed the storage ability of nanogel in defined storage conditions.

REFERENCES

1. Yousef H, Alhajj M, Sharma S. In: StatPearls [Internet]. Treasure Island (FL): StatPearls Publishing. 2023. Anatomy, Skin (Integument), Epidermis.
2. Czajkowska-Kośnik A, Szekalska M, Winnicka K. Nanostructured lipid carriers: A potential use for skin drug delivery systems. Pharmacol Reports [Internet]. 2019 Feb;71(1):156-66. Available from: https://doi.org/10.1016/j.pharep.2018.10.008
3. WHO. World Health Organization. 2017 [cited 2024 Feb 1]. Skin Cancer. Available from: https://www.who.int/uv/faq/skincancer/en/index1.html
4. Iqubal MK, Chaudhuri A, Iqubal A, Saleem S, Gupta MM, Ahuja A, *et al.* Targeted Delivery of Natural Bioactives and Lipid-nanocargos against Signaling Pathways Involved in Skin Cancer. Curr Med Chem. 2020 Nov 4;27:1-33.
5. Thompson K. Conventional therapies and emergent precision medicines for cystic fibrosis: challenges and opportunities. Pharm J. 2016;1-23.
6. Marchetti JM, de Souza MC, Marotta-Oliveira SS. Nanocarriers and Cancer Therapy: Approaches to Topical and Transdermal Delivery. In: Nanocosmetics and Nanomedicines. Berlin, Heidelberg: Springer Berlin Heidelberg; 2011. p. 269-86.
7. Iqubal MK, Kaur H, Md S, Alhakamy NA, Iqubal A, Ali J, *et al.* A technical note on emerging combination approach involved in the onconanotherapeutics. Drug Deliv. 2022;29(1):3197-212.
8. Nasim N, Sandeep IS, Mohanty S. Plant-derived natural products for drug discovery: current approaches and prospects. Nucl an Int J Cytol allied Top. 2022;65(3):399-411.
9. Banudevi S, Swaminathan S, Maheswari KU. Pleiotropic Role of Dietary Phytochemicals in Cancer: Emerging Perspectives for Combinational Therapy. Nutr Cancer. 2015;67(7):1021-48.
10. Ghayour N, Hosseini SMH, Eskandari MH, Esteghlal S, Nekoei AR, Hashemi Gahruie H, *et al.* Nanoencapsulation of quercetin and curcumin in casein-based delivery systems. Food Hydrocoll. 2019;87:394-403.
11. Mahajan H, Patil N. Nanoemulsion containing a synergistic combination of curcumin and quercetin for nose-To-brain delivery: *In vitro* and *in vivo* studies. Asian Pac J Trop Biomed. 2021;11(11):510-8.
12. Mansi K, Kumar R, Narula D, Pandey SK, Kumar V, Singh K. Microwave-Induced CuO Nanorods: A Comparative Approach between Curcumin, Quercetin and Rutin to Study Their Antioxidant, Antimicrobial and Anticancer Effects against Normal Skin Cells and Human Breast Cancer Cell Lines MCF-7 and T-47D. ACS Appl Bio Mater.2022;5(12): 5762-78.
13. El-rahman SNA. Curcumin (Curcuma longa) and quercetin nanoparticles as antimicrobial and anticancer agents. African J Biol Sci. 2021;17(1):205-19.
14. Nugraha AP, Yudianto DO, Anwar AA, Purnamasari AE, Mappananrang RA, Ramadhani NF, *et al.* Potential of Curcumin-Quercetin Loaded Nanostructured Lipid Carriers as Oral Squamous Cell Carcinoma Adjuvant Therapy by Downregulating AKT/PI3K Signaling Pathway. Res J Pharm Technol. 2022;15(11):5353-8.
15. Ravichandiran V, Masilamani K, Senthilnathan B, Maheshwaran A, Wong TW, Roy P. Quercetin-Decorated Curcumin Liposome Design for Cancer Therapy: *In vitro* and InVivo Studies. Curr Drug Deliv. 2016;14(8):78033.
16. Sandhiya V, Ubaidulla U. A review on herbal drug loaded into pharmaceutical carrier techniques and its evaluation process. Futur J Pharm Sci. 2020;6(1):1-16.
17. Sunoqrot S, Al-Debsi T, Al-Shalabi E, Hasan Ibrahim L, Faruqu FN, Walters A, *et al.* Bioinspired Polymerization of Quercetin to Produce a Curcumin-Loaded Nanomedicine with Potent Cytotoxicity and Cancer-Targeting Potential *in vivo*. ACS Biomater Sci Eng. 2019;5(11):6036-45.
18. Bagde A, Patel K, Mondal A, Kutlehria S, Chowdhury N, Gebeyehu A, *et al.* Combination of UVB Absorbing Titanium Dioxide and Quercetin Nanogel for Skin Cancer Chemoprevention. AAPS PharmSciTech. 2019 Jun 27; 20(6): 240.
19. Nan W, Ding L, Chen H, Khan FU, Yu L, Sui X, *et al.* Topical Use of Quercetin-Loaded Chitosan Nanoparticles Against Ultraviolet B Radiation. Front Pharmacol. 2015;9:1-11.
20. Ali H, Dixit S. Quercetin attenuates the development of 7, 12-dimethyl benz (a) anthracene (DMBA) and croton oil-induced skin cancer in mice. J Biomed Res. 2015 Apr;29(2):139-44.
21. Boots AW, Kubben N, Haenen GRM., Bast A. Oxidized quercetin reacts with thiols rather than with ascorbate: implication for quercetin supplementation. Biochem Biophys Res Commun. 2003 Aug;308(3):560-5.
22. LoTempio MM, Veena MS, Steele HL, Ramamurthy B, Ramalingam TS, Cohen AN, *et al.* Curcumin suppresses growth of head and neck squamous cell carcinoma. Clin Cancer Res. 2005 Oct 1 ; 11(19 Pt 1):6994-7002.
23. Vallianou NG, Evangelopoulos A, Schizas N, Kazazis C. Potential anticancer properties and mechanisms of action of curcumin. Anticancer Res. 2015 Feb;35(2):645-51.
24. Joshi P, Joshi S, Semwal D, Bisht A, Paliwal S, Dwivedi J, *et al.* Curcumin: An Insight into Molecular Pathways Involved in Anticancer Activity. Mini-Reviews Med Chem. 2021 Nov 23;21(17):2420-57.
25. Reyes-Farias M, Carrasco-Pozo C. The Anti-Cancer Effect of Quercetin: Molecular Implications in Cancer Metabolism. Int J Mol Sci. 2019 Jun 28;20(13):1-19.
26. ZHOU J, LI L, FANG L, XIE H, YAO W, ZHOU X, *et al.* Quercetin reduces cyclin D1 activity and induces G1 phase arrest in HepG2 cells. Oncol Lett. 2016 Jul;12(1):516-22.
27. Hu A, Huang JJ, Zhang JF, Dai WJ, Li RL, Lu ZY, *et al.* Curcumin induces G2/M cell cycle arrest and apoptosis of head and neck squamous cell carcinoma *in vitro* and *in vivo* through ATM/Chk2/p53-dependent pathway. Oncotarget. 2017;8(31):50747-60.

28. Harris Z, Donovan MG, Branco GM, Limesand KH, Burd R. Quercetin as an Emerging Anti-Melanoma Agent: A Four-Focus Area Therapeutic Development Strategy. Front Nutr. 2016 Oct 31;3:1-14.
29. Ming T, Tao Q, Tang S, Zhao H, Yang H, Liu M, *et al*. Curcumin: An epigenetic regulator and its application in cancer. Biomed Pharmacother. 2022 ;156:1-13.
30. Hasan AA, Tatarskiy V, Kalinina E. Synthetic Pathways and the Therapeutic Potential of Quercetin and Curcumin. Int J Mol Sci. 2022;23(22):1-20.
31. Vaz GR, Carrasco MCF, Batista MM, Barros PAB, Oliveira M da C, Muccillo-Baisch AL, *et al.* Curcumin and Quercetin-Loaded Lipid Nanocarriers: Development of Omega-3 Mucoadhesive Nanoemulsions for Intranasal Administration. Nanomater (Basel, Switzerland). 2022; 12(7):1-20.
32. Tilawat M, Bonde S. Curcumin and quercetin loaded nanocochleates gel formulation for localized application in breast cancer therapy. Heliyon. 2023;9(12):e22892.
33. Khosa A, Reddi S, Saha RN. Nanostructured lipid carriers for site-specific drug delivery. Biomed Pharmacother. 2018;103:598-613.
34. Carvajal-Vidal P, Fábrega MJ, Espina M, Calpena AC, García ML. Development of Halobetasol-loaded nanostructured lipid carrier for dermal administration: Optimization, physicochemical and biopharmaceutical behavior and therapeutic efficacy. Nanomedicine. 2019;20:102026.
35. Motawea A, Borg T, Abd El-Gawad AEGH. Topical phenytoin nanostructured lipid carriers: design and development. Vol. 44, Drug Development and Industrial Pharmacy. Taylor and Francis; 2018. 144-157 p.
36. Abdel-Salam FS, Mahmoud AA, Ammar HO, Elkheshen SA. Nanostructured lipid carriers as semisolid topical delivery formulations for diflucortolone valerate. J Liposome Res. 2017;27:41-55.
37. Iqubal MK, Kamal A, Iqubal A, Imran M, Ali J, Baboota S. Development and Validation of a Robust HPLC Method for Simultaneous Estimation of 5-Fluorouracil and Resveratrol and its Application in the Engineered Nanostructured Lipid Carrier. Curr Anal Chem. 2021;17(3):385-95.
38. Iqubal MK, Iqubal A, Imtiyaz K, Rizvi MMA, Gupta MM, Ali J, *et al.* Combinatorial lipidnanosystem for dermal delivery of 5-fluorouracil and resveratrol against skin cancer: Delineation of improved dermatokinetics and epidermal drug deposition enhancement analysis. Eur J Pharm Biopharm. 2021; 163:223-39.
39. Qamar Z, Ashhar MU, Annu, Qizilibash FF, Sahoo PK, Ali A, *et al.* Lipid nanocarrier of selegiline augmented anti-Parkinson's effect via P-gp modulation using quercetin. Int J Pharm. 2021;609:121131.
40. Negi LM, Jaggi M, Talegaonkar S. Development of protocol for screening the formulation components and the assessment of common quality problems of nano-structured lipid carriers. Int J Pharm. 2014;461(1-2):403-10.
41. Khan SA, Rehman S, Nabi B, Iqubal A, Nehal N, Fahmy UA, *et al.* Boosting the Brain Delivery of Atazanavir through Nanostructured Lipid Carrier-Based Approach for Mitigating NeuroAIDS. Pharmaceutics. 2020;12:1-26.
42. Iqbal MA, Md S, Mustafa G, Kumar M, Baboota S, Sahni JK, *et al.* Formulation, optimization and evaluation of nanostructured lipid carrier system of acyclovir for topical delivery. J Bionanoscience. 2014;8(4):235-47.
43. Iqubal MK, Iqubal A, Anjum H, Gupta MM, Ali J, Baboota S. Determination of *in vivo* virtue of dermal targeted combinatorial lipid nanocolloidal based formulation of 5fluorouracil and resveratrol against skin cancer. Int J Pharm. 2021;610:121179.
44. Rajinikanth PS, Chellian J. Development and evaluation of nanostructured lipid carrierbased hydrogel for topical delivery of 5-fluorouracil. Int J Nanomedicine. 2016;11:5067-77.
45. Singh A, Iqubal MK, Mittal S, Qizilbash FF, Sartaz A, Kumar S, *et al.* Designing and evaluation of dermal targeted combinatorial nanostructured lipid carrier gel loaded with curcumin and resveratrol for accelerating cutaneous wound healing. Part Sci Technol. 2023; 1-19.
46. Gupta DK, Aqil M, Ahad A, Imam SS, Waheed A, Qadir A, *et al.* Tailoring of berberine loaded transniosomes for the management of skin cancer in mice. J Drug Deliv Sci Technol. 2020;60:102051.
47. Safwat MA, Soliman GM, Sayed D, Attia MA. Fluorouracil-Loaded Gold Nanoparticles for the Treatment of Skin Cancer: Development, *in vitro* Characterization and *in vivo* Evaluation in a Mouse Skin Cancer Xenograft Model. Mol Pharm. 2018;15(6):2194-205.
48. Negi P, Singh B, Sharma G, Beg S, Katare OP. Biocompatible lidocaine and prilocaine loaded-nanoemulsion system for enhanced percutaneous absorption: QbD-based optimisation, dermatokinetics and *in vivo* evaluation. J Microencapsul. 2015;32(5):419-31.
49. Raza K, Singh B, Lohan S, Sharma G, Negi P, Yachha Y, *et al.* Nano-lipoidal carriers of tretinoin with enhanced percutaneous absorption, photostability, biocompatibility and antipsoriatic activity. Int J Pharm. 2013;456(1):65-72.
50. Balla E, Zamboulis A, Klonos P, Kyritsis A, Barmpalexis P, Bikiaris DN. Synthesis of novel interpenetrated network for ocular co-administration of timolol maleate and dorzolamide hydrochloride drugs. Int J Pharm. 2023;646:123439.
51. Hurler J, Engesland A, Kermany BP, Kalko-Basnet N. Improved Texture Analysis for Hydrogel Characterization: Gel Cohesiveness, Adhesiveness and Hardness. J Appl Polym Sci. 2011;116(5):180-8.
52. Chauhan I, Yasir M, Verma M, Singh AP. Nanostructured Lipid Carriers: A Groundbreaking Approach for Transdermal Drug Delivery. Adv Pharm Bull. 2020;10(2):150-65.
53. Balogh B, Pető Á, Haimhoffer Á, Sinka D, Kósa D, Fehér P, *et al.* Formulation and Evaluation of Different Nanogels of Tapinarof for Treatment of Psoriasis. Gels. 2024;10(11):675.
54. Raszewska-Famielec M, Flieger J. Nanoparticles for Topical Application in the Treatment of Skin Dysfunctions-An Overview of Dermo-Cosmetic and Dermatological Products. Int J Mol Sci. 2022;23(24):1-54.
55. Ngan CL oon., Basri M, Lye FF an., Fard Masoumi HR ez., Tripathy M, Karjiban RA bed., *et al.* Comparison of process parameter optimization using different designs in nanoemulsion-based formulation for transdermal delivery of fullerene. Int J Nanomedicine. 2014;9:4375-86.
56. Olerile LD, Liu Y, Zhang B, Wang T, Mu S, Zhang J, *et al.* Near-infrared mediated quantum dots and paclitaxel co-loaded nanostructured lipid carriers for cancer theragnostic. Colloids Surfaces B Biointerfaces. 2017 Feb ;150:121-30.
57. Patwekar SL, Pedewad SR, Gattani S. Development and evaluation of nanostructured lipid carriers-based gel of isotretinoin. Part Sci Technol. 2018;36(7):832-43.
58. Loo C, Basri M, Ismail R, Lau H, Tejo B, Kanthimathi M, *et al.* Effect of compositions in nanostructured lipid carriers (NLC) on skin hydration and occlusion. Int J Nanomedicine. 2013;8:13-22.
59. Siddalingam R, Chidambaram K. Topical nano-delivery of 5-fluorouracil : Preparation and characterization of water-in-oil nanoemulsion. 2016;15:2311-9.
60. Bose S, Du Y, Takhistov P, Michniak-Kohn B. Formulation optimization and topical delivery of quercetin from solid lipid based nanosystems. Int J Pharm. 2013 ; 441(1- 2):56-66.
61. Khogta S, Patel J, Barve K, Londhe V. Herbal nano-formulations for topical delivery. J Herb Med. 2020 ;20:100300.

Cite this article: Iqubal MK, Shadab Md, Ali J, Baboot S. Formulation and Evaluation of Lipid Nanogel Loaded with Quercetin and Curcumin for Improvement of Topical Bioavailability. Indian J of Pharmaceutical Education and Research. 2025;59(2):585-601.